

Freezing transitions of Brownian particles in confining potentials

Gabriel Mercado-Vásquez¹, Denis Boyer¹, and Satya N. Majumdar²

¹ Instituto de Física, Universidad Nacional Autónoma de México, Mexico City 04510, Mexico

² LPTMS, CNRS, Univ. Paris-Sud, Université Paris-Saclay, 91405 Orsay, France

Abstract. We study the mean first passage time (MFPT) to an absorbing target of a one-dimensional Brownian particle subject to an external potential $v(x)$ in a finite domain. We focus on the cases in which the external potential is confining, of the form $v(x) = k|x - x_0|^n/n$, and where the particle's initial position coincides with x_0 . We first consider a particle between an absorbing target at $x = 0$ and a reflective wall at $x = c$. At fixed x_0 , we show that when the target distance c exceeds a critical value, there exists a nonzero optimal stiffness k_{opt} that minimizes the MFPT to the target. However, when c lies below the critical value, the optimal stiffness k_{opt} vanishes. Hence, for any value of n , the optimal potential stiffness undergoes a continuous “freezing” transition as the domain size is varied. On the other hand, when the reflective wall is replaced by a second absorbing target, the freezing transition in k_{opt} becomes discontinuous. The phase diagram in the (x_0, n) -plane then exhibits three dynamical phases and metastability, with a “triple” point at $(x_0/c \simeq 0.17185, n \simeq 0.39539)$. For harmonic or higher order potentials ($n \geq 2$), the MFPT always increases with k at small k , for any x_0 or domain size. These results are contrasted with problems of diffusion under optimal resetting in bounded domains.

Keywords: Brownian motion, potential landscape, optimal potential, stochastic searches, resetting processes

1. Introduction

The theory of first passage processes is concerned with the statistical properties of the time it takes for a stochastic process to reach a specific configuration or site for the first time [1–3]. The first passage time (FPT) is of primary relevance in problems across many areas of science, ranging from chemical reaction kinetics [4–7], neuronal science [8, 9], animal foraging [10, 11], or finance [12]. In many situations, the motion of a diffusive entity is restricted by the surroundings of the medium or some particular limits. The introduction of boundaries has many implications on the particle dynamics and the statistical properties of the FPT [2, 13]. For simple diffusive processes, it is well-known that the mean first passage time (MFPT) to an absorbing target is finite in a bounded domain, unlike in the open geometry where it is infinite [2]. At the biological level the presence of boundaries can influence the completion of vital processes: gene transcription is strongly controlled by the geometry of the medium; in crowded environments composed of many obstacles, the time at which a gene is activated is extremely sensitive to changes in the initial position of the transcription factors [13, 14]. To achieve their biological function, certain substances must diffuse inside the cell volume until they escape from the confinement through a narrow window [15]. Red blood cells are oxygenated once the oxygen reaches the cell wall and diffuses within the cell interior [16]. The presence of boundaries can also affect reaction kinetics when there are more than one target site [17].

Placing hard obstacles in the bulk of the system is not the only way to restrict the motion of particles; external forces can also serve for this purpose. In the celebrated Kramers problem [18, 19], a Brownian particle is trapped in a potential well; to reach another (deeper) well the particle must surpass a potential barrier with the assistance of thermal fluctuations. In a polymer chain, for instance, the two ends of the chain have to overcome the harmonic potential between them in order to react [4]. Potential barriers strongly influence the first passage statistics of diffusive systems. In particular, the shape of the potential can have unexpected consequences on the rate at which the FPT probability density decays at large times [20].

As the efficiency of a search process can be measured through the MFPT, an important question one may ask is: which shape should an external potential have in order to minimize the time taken by a particle to encounter its target? This question has been addressed in different contexts. For instance, a piece-wise linear potential fluctuating in time between two different barrier heights produces a stochastic resonant activation that can lower the MFPT compared to the time taken with the average potential [21]. In the context of static potentials, the introduction of a high but narrow barrier near a hard wall markedly reduces the MFPT to a target site located on the other side of the barrier [22, 23]. Extensions have also considered subdiffusive processes [24]. When the target is randomly placed at a position chosen from a given distribution, the optimal potential shape can be deduced from a variational calculation [25].

In recent years, it has been shown that random searches in equilibrium can be

further optimized by driving the searcher out of equilibrium. One way of doing this is for instance through resetting, *i.e.*, by means of stochastic interruptions of the motion that bring the searcher back to a particular position of space, from which movement starts afresh [26]. These interruptions can benefit the search process by cutting off those fruitless trajectories that move away from the target position. The MFPT can be minimized with respect to the resetting rate for a variety of background processes, such as Brownian motion [27,28] or Lévy flights [29]. Stochastic processes with resetting also exhibit interesting features such as the emergence of non-equilibrium steady states (NESS) [27,30,31], whose relaxation dynamics is quite peculiar [32–34].

The stationary distribution of a Brownian motion with diffusion constant D under resetting at finite rate r resembles a Boltzmann-Gibbs steady state with an effective potential of the form $k|x - x_0|$, where x_0 is the resetting position and $k = \sqrt{r/D}$ [35]. However, motion under resetting is markedly different from a Langevin dynamics in this effective potential. On a semi-infinite line with an absorbing wall located at the origin, it is also possible to minimize with respect to k the MFPT given by the Kramer's theory and the above piece-wise linear potential. It is found that the MFPT of the particle under resetting at the optimal rate is lower than the optimal MFPT in the Kramers case [35,36].

Nevertheless, in finite domains, resetting does not always represent an efficient search strategy but can be detrimental instead. Depending on the location of the resetting position with respect to the boundaries, resetting can either decrease or increase the MFPT that would be obtained with simple diffusion [37,38]. As x_0 is varied away from the target, the optimal resetting rate r_{opt} typically undergoes a continuous "freezing" transition from $r_{\text{opt}} > 0$ to $r_{\text{opt}} = 0$ (equivalent to free diffusion) at a particular critical position x_c . If the diffusive particle is additionally subject to an external potential, the interplay between resetting and the crossing of potential barriers (in finite or infinite intervals) can also produce transitions where the advantage of resetting vanishes [39–41]. In situations where the potential attracts the particle toward the target, strong enough potentials can also suppress the benefit of resetting to the initial position [41,42]. In those cases, there are ranges of values of the potential strength for which r_{opt} vanishes. These intriguing transitions have been studied for resetting problems, sometimes in combination with external potentials as mentioned above. However, to our knowledge, a systematic analysis of random search optimization in finite intervals using external potentials only (without resetting) is still lacking.

We aim in this work to study target encounter optimization in the presence of confining potentials in finite domains, and to contrast with the results that are known for resetting problems in similar geometries. The motion of the particle is confined within a one-dimensional interval $[0, c]$ in two different set-ups: In set-up I (see Fig. 1-left), an absorbing boundary is located at the origin whereas a reflective wall is placed at $x = c$. In set-up II (Fig. 1-right), both boundaries are absorbing. We consider here external potentials that are minimum at a position x_0 , of the form $v(x) = k|x - x_0|^n/n$, where $n > 0$, $k \geq 0$. The limiting case $n \rightarrow 0$ corresponds to the logarithmic potential.

We are mainly interested in the effects that the parameters k , x_0 and n have on the mean first passage time properties of the system. Although this problem is directly related to the classical Kramers' problem, it exhibits rich behaviours that are not observed in unbounded domains, or even for free diffusion with stochastic resetting.

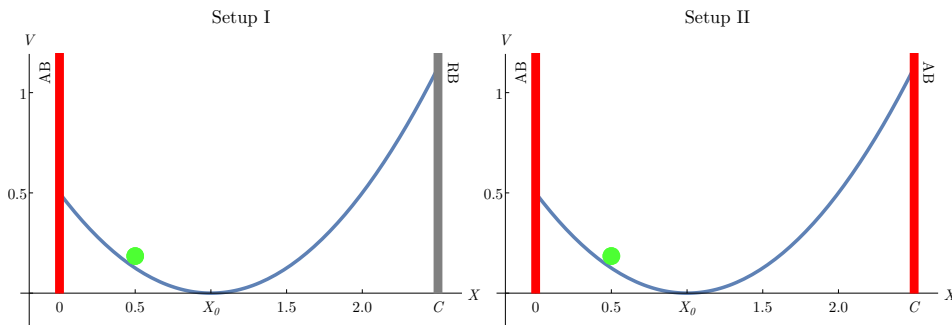


Figure 1. The two set-ups investigated here. A Brownian particle (green point) is subject to a potential $v(x)$ with a minimum at $x_0 = 1$. In set-up I, an absorbing boundary (AB) is placed at the origin, whereas a reflective boundary (RB) is placed at c . In set-up II, both walls are absorbing.

This article is organized as follows: In Section 2 we compute the mean time needed for a Brownian particle subject to a potential $v(x)$ to reach a target with the two different boundary conditions. Section 3 is devoted to the investigation of set-up I. We analyze the expression of the MFPT for a particle starting from x_0 as a function of the potential stiffness k , finding that, when x_0/c is below a critical value, the MFPT can be minimized at a non-zero stiffness k_{opt} , whereas above the critical value, the mean search time is optimized by setting $k = 0$. In section 3.2, we compare this "freezing" transition for k_{opt} , which is continuous, to the similar transition that occurs in this geometry for the problem of free diffusion under resetting. In Section 4 we compute and analyze the MFPT for the set-up II (or the mean exit time of the particle from the interval $[0, c]$). We observe qualitatively different behaviours: due to metastability effects, the transition in k_{opt} at fixed n is discontinuous as x_0/c crosses a transition point, at least for $n > 0.39539\dots$. Finally, we discuss our findings in Section 5.

2. General set-up and the solution

In this section we shall recall some well-known results in the literature [43, 44]. This will help set up our notations and the analysis to follow in subsequent sections. The evolution of a Brownian particle with position $X(t)$ in a potential $V(X)$ is given by the over-damped Langevin equation:

$$\frac{dX(t)}{dt} = -\frac{V'(X(t))}{\Gamma} + \sqrt{2D}\xi(t), \quad (1)$$

where Γ is the friction coefficient, $\xi(t)$ a Gaussian white noise of zero mean and correlations $\langle \xi(t)\xi(t') \rangle = \delta(t - t')$, and D the diffusion coefficient. The particle is confined in a domain of size C , or $0 \leq X \leq C$.

In the following it is convenient to introduce the dimensionless space and time variables $x = X/L$ and $t/(L^2/D)$ (which we re-note as t), where L is an arbitrary length. If $V(X)$ has a single minimum, L can be chosen as the distance X_0 between the potential minimum and the target placed at $X = 0$. Alternatively, L can be set to the domain size C . The re-scaled potential is given by $v(x) = V(xL)/(\Gamma D) = V(xL)/(k_B T)$. The re-scaled domain size, potential minimum position and particle's initial position are denoted as $c = C/L$, $x_0 = X_0/L$ and $x_i = X_i/L$, respectively. In these dimensionless variables, the Langevin equation (1) reduces to

$$\frac{dx}{dt} = -v'(x) + \sqrt{2}\eta(t) \quad (2)$$

where $\langle \eta(t) \rangle = 0$ and $\langle \eta(t)\eta(t') \rangle = \delta(t - t')$.

We define the survival probability $Q(x_i, t)$ as the probability that the diffusing particle has not been absorbed yet at time t , given the initial position x_i . We re-note $x_i = x$ in the following. This probability satisfies the backward Fokker-Planck equation (see *e.g.* [43])

$$\frac{\partial Q(x, t)}{\partial t} = \frac{\partial^2 Q(x, t)}{\partial x^2} - v'(x) \frac{\partial Q(x, t)}{\partial x}. \quad (3)$$

Defining the Laplace transform $\tilde{Q}(x, s) = \int_0^\infty dt e^{-st} Q(x, t)$ and integrating by parts, Eq. (3) can be recast as

$$\frac{\partial^2 \tilde{Q}(x, s)}{\partial x^2} - v'(x) \frac{\partial \tilde{Q}(x, s)}{\partial x} - s\tilde{Q}(x, s) = -1, \quad (4)$$

where we have imposed the initial condition $Q(x, t = 0) = 1$ for all $0 < x < c$.

As the motion of the particle is confined by the potential, the problem allows us to compute the mean first passage time (MFPT), which is the mean time at which the particle reaches an absorbing boundary for the first time. This quantity can be easily computed knowing the Laplace transform of the survival probability through the usual relation

$$T(x) = \int_0^\infty Q(x, t) dt = \tilde{Q}(x, s = 0). \quad (5)$$

Therefore, taking $s = 0$ in Eq. (4) we obtain the equation for the MFPT $T(x)$ for a Brownian particle in the presence of the potential $v(x)$

$$\frac{\partial^2 T(x)}{\partial x^2} - v'(x) \frac{\partial T(x)}{\partial x} = -1, \quad (6)$$

whose general solution is obtained by direct integration as

$$T(x) = A \int_0^x dy e^{v(y)} + B - \int_0^x dy \int_0^y dz e^{v(y)-v(z)}. \quad (7)$$

The first two terms solve the homogeneous equation whereas the last one is the particular inhomogeneous solution. The constants of integration A and B are determined by the boundary conditions. In the two set-ups considered here, an absorbing target is placed at the origin, therefore

$$T(x = 0) = 0, \quad (8)$$

as a particle starting at $x = 0$ is immediately absorbed. Hence, we have $B = 0$ in Eq. (7), or

$$T(x) = A \int_0^x dy e^{v(y)} - \int_0^x dy \int_0^y dz e^{v(y)-v(z)}. \quad (9)$$

In set-up I, a reflective wall is placed at $x = c$, which implies

$$\left. \frac{\partial T(x)}{\partial x} \right|_{x=c} = 0. \quad (10)$$

This boundary condition gives, from Eq. (9),

$$A_I = \int_0^c dz e^{-v(z)} \quad (11)$$

and the MFPT for set-up I,

$$T_I(x) = \int_0^x dy \int_y^c dz e^{v(y)-v(z)}, \quad (12)$$

a result obtained in [4], for instance.

In set-up II, another absorbing target is placed at $x = c$ and the boundary condition becomes

$$T(x = c) = 0. \quad (13)$$

From Eq. (9), the constant is now given by

$$A_{II} = \frac{\int_0^c dy \int_0^y dz e^{v(y)-v(z)}}{\int_0^c dy e^{v(y)}} \quad (14)$$

and the solution by

$$T_{II}(x) = \frac{\int_0^c dy \int_0^y dz e^{v(y)-v(z)}}{\int_0^c dy e^{v(y)}} \int_0^x dy e^{v(y)} - \int_0^x dy \int_0^y dz e^{v(y)-v(z)}, \quad (15)$$

as obtained in [44], for instance.

In the following we consider a potential of the form $v(x) = k|x-x_0|^n/n$, where $n > 0$ and $k \geq 0$, *i.e.*, with a minimum at x_0 . The dimensionless parameter k is related to the dimensional stiffness K through the expression $k = KL^n/(k_B T)$. With this potential, the general expression of the MFPT in Eq. (9) can be recast as

$$T(x) = A \int_0^x dy e^{\frac{k}{n}|y-x_0|^n} - \int_0^x dy \int_0^y dz e^{\frac{k}{n}(|y-x_0|^n - |z-x_0|^n)}, \quad (16)$$

where A takes the value

$$A_I = \int_0^c dz e^{-\frac{k}{n}|z-x_0|^n} \quad (17)$$

with the reflective boundary at c , or

$$A_{II} = \frac{\int_0^c dy \int_0^y dz e^{\frac{k}{n}(|y-x_0|^n - |z-x_0|^n)}}{\int_0^c dy e^{\frac{k}{n}|y-x_0|^n}} \quad (18)$$

in the case of an absorbing boundary at c .

3. Set-up I: absorbing/reflective boundaries

In this section we choose $L = X_0$ as the characteristic length of the system, hence, the dimensionless space variable is $x = X/X_0$ and $x_0 = 1$. In order to analyze the behaviour of the MFPT as a function of the potential order n and its stiffness k , we consider the case in which the initial position of the particle coincides with the minimum of the potential ($x = 1$). In this case, the MFPT will be simply denoted as T_I and from Eqs. (16) and (17), it can be written as

$$T_I = \int_0^1 dy \int_y^c dz e^{\frac{k}{n}(|y-1|^n - |z-1|^n)}. \quad (19)$$

The reflective wall is obviously placed further to the right side of the initial position, therefore $c \geq 1$.

3.1. Optimal potential stiffness k

Let us examine the MFPT as a function of the stiffness k of the potential for different locations c of the reflective wall (n being fixed). We consider two opposite limits: (i) When the wall is at $c = 1$, *i.e.*, at the initial position of the particle, the particle cannot move to the right and only moves to the left. As k increases, it has to climb a higher barrier to reach the target at 0 and hence the MFPT will increase monotonically with k . The stiffer the barrier, more time is needed to reach the target. (ii) The second is the opposite limit when $c \rightarrow \infty$, *i.e.*, the wall is far away to the right. In this case, when $k \rightarrow 0$ (free diffusion), the MFPT is infinite since there are trajectories that wander away to infinity in the direction opposite to the target. On the other hand, when $k \rightarrow \infty$ (extremely stiff potential centered around $x = 1$), the particle gets fully localised at $x = 1$ and is prevented to reach the target, hence the MFPT again diverges. Thus the MFPT, as a function of k (for fixed $c \rightarrow \infty$) diverges at the two limits $k \rightarrow 0$ and $k \rightarrow \infty$. Consequently, it must have a minimum at some intermediate finite value $k = k_{\text{opt}}$. As c varies from 1 to ∞ , the above reasoning suggests that there is a likely critical value c^* at which the situation changes from (i) to (ii), *i.e.*, the MFPT vs. k curve must change from a monotonically increasing [situation (i)] to a non-monotonic behavior with a minimum at k_{opt} [situation (ii)]. Therefore, at fixed shape parameter n , the optimal potential stiffness undergoes a continuous “freezing” transition with the domain size, where the optimal stiffness is the “order parameter” and c the “control parameter”.

The analysis of Eq. (19) confirms this scenario, as shown by Figs. 2a and 2b. The exact value of c^* depends on the exponent n and corresponds to the point at which the slope of T_I at $k = 0$ changes from positive to negative values, *i.e.*,

$$\left. \frac{\partial T_I(k, c^*)}{\partial k} \right|_{k=0} = 0. \quad (20)$$

Taking the derivative of Eq. (19) we get

$$\left. \frac{\partial T_I(k, c)}{\partial k} \right|_{k=0} = \frac{1}{n} \int_0^1 dy \int_y^c dz (|y-1|^n - |z-1|^n) = \frac{c-1 - (c-1)^{n+1} + \frac{n}{n+2}}{n(n+1)}. \quad (21)$$

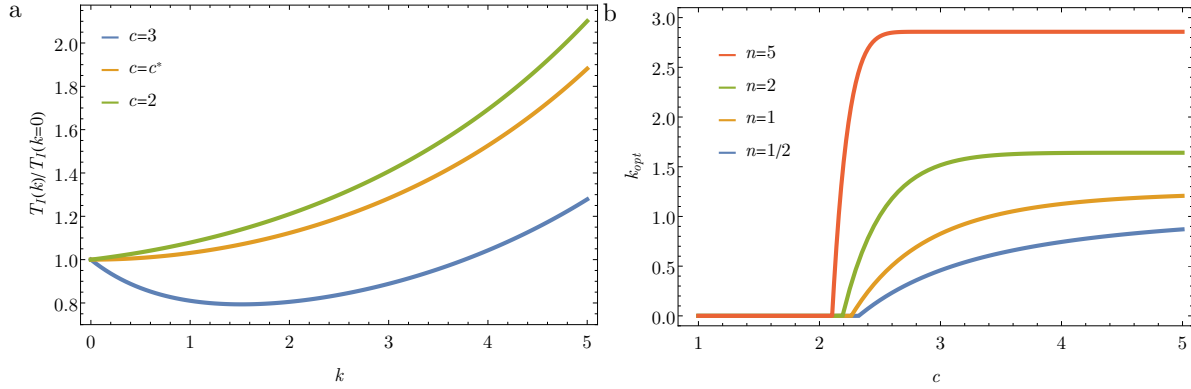


Figure 2. Searches starting from $x_0 = 1$. (a) Normalized mean first passage time $T_I(k)/T_I(k=0)$ as a function of the potential stiffness for a harmonic potential ($n = 2$) and different values of the domain size c . (b) Optimal potential stiffness k_{opt} as a function of the domain size c for different potential exponent n .

Setting the above expression equal to zero we find

$$c^* = 1 + \ell, \quad (22)$$

where ℓ is the positive root of the equation

$$\ell^{n+1} - \ell - \frac{n}{n+2} = 0. \quad (23)$$

In the particular case $n = 1$, this equation is easily solved as

$$c^*(n = 1) = \frac{3 + \sqrt{7/3}}{2} = 2.26376 \dots \quad (24)$$

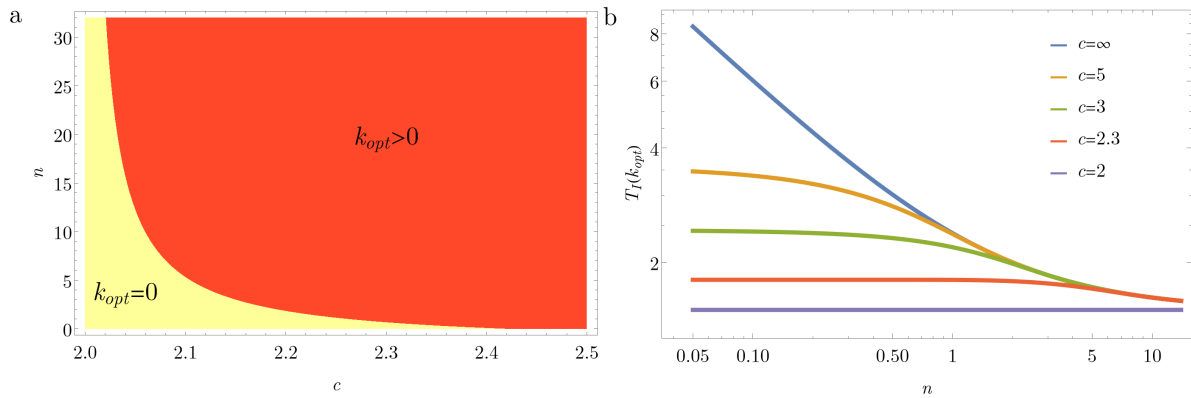


Figure 3. Searches starting from $x_0 = 1$. (a) Phase diagram in the (c, n) -plane. In the red area the MFPT is minimum at a potential stiffness $k_{opt} > 0$, whereas in the yellow region simple diffusion ($k = 0$) is optimal. (b) MFPT evaluated at the optimal potential stiffness k_{opt} as a function of n for several values of c , including the case of the semi-infinite line $c = \infty$.

The value of the critical domain size c^* decreases with n , as illustrated by the diagram 3a showing the two dynamical phases. The value of c^* is maximal when $n \rightarrow 0$, and minimal at $n = \infty$. In the limit $n \rightarrow \infty$, Eq. (22) gives $c^*(n \rightarrow \infty) \approx$

$2 + \ln(2)/n + O(1/n^2)$, therefore, $c^*(n = \infty) = 2$. Conversely, in the limit $n \rightarrow 0$, the equation for the root ℓ simplifies to $\ell \ln(\ell) = 1/2 + O(n)$, whose solution leads to the non-trivial value $c^*(n \rightarrow 0) = 2.42153\dots$

In Fig. 3b, we observe that the optimal MFPT, or $T_I(k = k_{\text{opt}})$, is a decreasing function of n for any $c > 2$. Therefore the best possible potential is the one corresponding to $n \rightarrow \infty$, or $v(x) = 0$ for $x < 2$ and $v(x) = \infty$ for $x > 2$, which is equivalent to having a freely diffusing particle in a domain of size 2 (or $2X_0$ in the original coordinate). We show in Fig. 4 the shape of several optimal potentials $v^*(x) = k_{\text{opt}}|x - 1|^n/n$ for different values of the potential exponent n , in a domain of size 2.5.

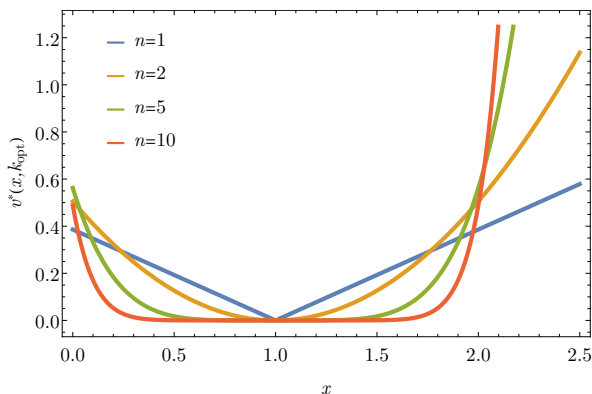


Figure 4. Potential $v(x) = k|x - 1|^n/n$ as a function of x , evaluated at the optimal potential stiffness k_{opt} for different values of n . The domain size is fixed to $c = 2.5$.

3.2. Comparison with optimal resetting

The above results show the existence of a critical domain size c^* below which the optimal stiffness k_{opt} freezes to the value 0. For completeness and to provide a coherent picture, we revisit in this section a problem where a similar transition was found in bounded domains, for a free Brownian particle subject to resetting to the initial position. Following [26, 27, 38], let us consider a Brownian particle that diffuses in the interval $[0, c]$ (where $v(x) = 0$) and is reset to its initial position at exponentially distributed times with mean $1/r$. The boundaries at $x = 0$ and c are absorbing and reflective, respectively, like in set-up I. Whereas diffusion in a static confining potential $v(x)$ describes an equilibrium process, resetting violates local detailed balance and generates dynamically a non-equilibrium steady state with an effective linear potential similar to the case $n = 1$ and where k is substituted by \sqrt{r} [35]. Although the results shown below have already been developed previously under some form [28, 42], we would like to emphasize that the MFPT in the resetting problem has a very different behaviour with respect to the domain size.

The Laplace transform of the survival probability of a process under stochastic resetting, $\tilde{Q}_r(x, s)$, can be related to the same quantity for the process in the absence

of resetting, $\tilde{Q}_0(x, s)$, through the relation [28]

$$\tilde{Q}_r(x, s) = \frac{\tilde{Q}_0(x, s+r)}{1 - r\tilde{Q}_0(x, s+r)}, \quad (25)$$

where the resetting position coincides with the initial position x . The survival probability $\tilde{Q}_0(x, s)$ for a diffusive particle solves Eq. (4) with the potential $v(x) = 0$, and satisfies the boundary conditions $Q(x = 0, t) = 0$ and $\partial_x Q(x, t)|_{x=c} = 0$. Hence $\tilde{Q}_0(x, s)$ is given by

$$\tilde{Q}_0(x, s) = \frac{1}{s} - \frac{\cosh \sqrt{s}(c-x)}{s \cosh \sqrt{sc}}. \quad (26)$$

Inserting the relation (26) into (25) and using (5), one obtains the MFPT under resetting, $T_r(x)$:

$$T_r(x) = \frac{\cosh \sqrt{rc}}{r \cosh \sqrt{r}(c-x)} - \frac{1}{r}. \quad (27)$$

(It is implicit in the above expression that the resetting rate is expressed in units of D/L^2 , the inverse of the characteristic time introduced at the beginning of section 2.)

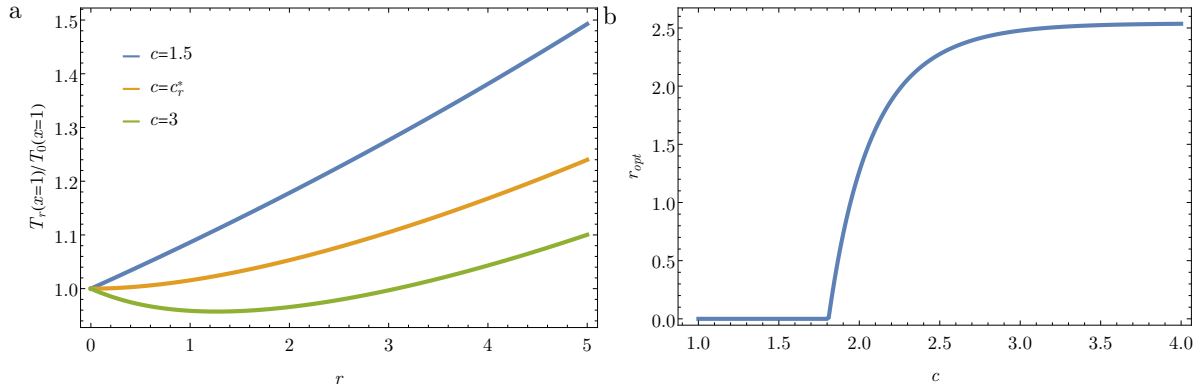


Figure 5. Brownian searches starting from $x = 1$ and subject to stochastic resetting, in set-up I. (a) Mean first passage time as a function of the re-scaled resetting rate r for different values of the domain size c . (b) Optimal resetting rate r_{opt} as a function of the domain size.

Fixing the resetting position to $x = 1$, we see in Fig. 5a-b that T_r exhibits a behaviour with respect to r similar to that of T_I with k . When the domain size is below a critical value c_r^* , resetting does not improve target search and the minimum of the MFPT is reached at $r = 0$ (free diffusion), whereas for $c \geq c_r^*$ the MFPT is optimized at a resetting rate r_{opt} which varies continuously from 0. The critical size c_r^* is determined from the condition

$$\left. \frac{\partial T_r(r, c_r^*)}{\partial r} \right|_{r=0} = 0, \quad (28)$$

which gives, from Eq. (27),

$$c_r^* = \frac{1}{1 - \frac{1}{\sqrt{5}}} = 1.80902 \dots < 2 \quad (29)$$

a result previously derived in [42]. In dimensional units, the critical domain size reads

$$C_r^* = \frac{X_0}{1 - \frac{1}{\sqrt{5}}}. \quad (30)$$

The value of c_r^* is lower than the critical domain size c^* in the equilibrium case with any confining potential $v(x) = k|x - 1|^n/n$. Hence, resetting has a negative effect on the MFPT over a smaller interval of domain sizes. In addition, as shown by Fig. 6, searches at the optimal resetting rate r_{opt} are faster (for c above c_r^*) than their counterparts that use an optimal potential with $n = 1$, or $v^*(x) = k_{\text{opt}}|x - 1|$. This result agrees with the unbounded domain case without the reflective wall [35]. We also display for comparison the case of simple diffusion ($v(x) = 0$).

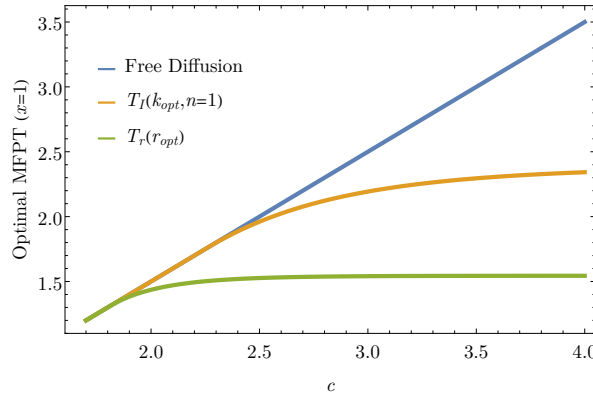


Figure 6. Optimal mean first passage time as a function of the domain size for a diffusive particle in an external potential $v(x) = k|x - 1|$ with $k = k_{\text{opt}}(c)$, or subject to stochastic resetting to the initial position $x = 1$, at the optimal resetting rate $r_{\text{opt}}(c)$. The free diffusion case also in shown.

4. Set-up II: absorbing/absorbing boundaries

We now turn to the case of two absorbing boundaries. For convenience we now set the characteristic length L equal to the domain size C . Hence, $c = 1$ and the dimensionless space variable is $x = X/C$, which is comprised in the interval $[0, 1]$. Again, we consider a particle with initial position at the minimum of the potential ($x = x_0$), which can be varied in $[0, 1]$.

Setting $c = 1$ in Eq. (16) and (18) we obtain

$$T_{II}(x_0) = \frac{\int_0^1 dy \int_0^y dz e^{\frac{k}{n}(|y-x_0|^n - |z-x_0|^n)}}{\int_0^1 dy e^{\frac{k}{n}|y-x_0|^n}} \int_0^{x_0} dy e^{\frac{k}{n}|y-x_0|^n} - \int_0^{x_0} dy \int_0^y dz e^{\frac{k}{n}(|y-x_0|^n - |z-x_0|^n)}. \quad (31)$$

We investigate how the position x_0 affects the behavior of the MFPT.

4.1. Optimal potential stiffness k

In set-up I, we have seen that above a critical value of the domain size, the potential expedites target encounter as the stiffness k increases from 0. Since the domain size was

given in units of x_0 (the distance between the potential minimum and the target located at the origin), the above conclusion is equivalent to say that, if the domain size is fixed to unity, the presence of the confining potential can accelerate target encounter if the distance x_0 is smaller than $x_c = 1/c^*$. If $x_0 > x_c$, on the contrary, a weak potential delays search. Here, one would expect a similar behaviour if one sets x_0 close to any of the two absorbing boundaries. There should exist a x_c such that, in the intervals $0 < x_0 < x_c$ and $1 - x_c < x_0 < 1$, the MFPT decreases with k at small k , whereas it increases in $[x_c, 1 - x_c]$. A similar situation is actually encountered (with respect to r) in the resetting problem with two absorbing boundaries [38].

The behavior of Eq. (31) with x_0 is actually quite different from the single target case and the scenario sketched above. Due to the symmetry of the problem, let us focus on the case $x_0 \in [0, 1/2]$. There generally exist not two, but three distinct regions in this interval for the MFPT (see Fig. 7a):

(i) When $0 < x_0 < x_c$, the derivative $\partial_k T_{II}|_{k=0}$ is < 0 and the equation $\partial_k T_{II}(k) = 0$ has a root $k^* > 0$, where T_{II} reaches its absolute minimum. Therefore $k_{\text{opt}} = k^*$.

(ii) When $x_c < x_0 < x_m$, the derivative $\partial_k T_{II}|_{k=0}$ is > 0 , but $T_{II}(k)$ vs. k has two local minima: one at $k = 0$ and the other at $k = k^*$ where $\partial_k T_{II}(k^*) = 0$. In this region, $T_{II}(k^*) < T_{II}(0)$, thus the optimal parameter is still $k_{\text{opt}} = k^*$, while $k = 0$ is metastable.

(iii) When $x_0 > x_m$, $T_{II}(0)$ is the absolute minimum ($k_{\text{opt}} = 0$). Thus x_m can be deduced by solving $T_{II}(k^*) = T_{II}(0)$.

Figure 7b displays, for the particular case $n = 1.5$, how the interval $[0, 1]$ is subdivided into five regions where the three phases above are observed. Fig. 7c shows the whole phase diagram in the (x_0, n) -plane, which we discuss qualitatively. The critical line $x_c(n)$ that limits the first region is obtained analytically (see below), whereas the line $x_m(n)$ is obtained from numerical minimization of Eq. (31). Surprisingly, when $n \geq 2$, $x_c = 0$, namely, the region (i) disappears. This means that for harmonic or higher order potentials, the MFPT always increases with k at small k , for any values of x_0 in the interval.

Notably, when the starting position x_0 crosses the boundary from region (ii) to (iii) at n fixed, the optimal stiffness k_{opt} undergoes a discontinuous "first order" transition, with an abrupt jump from the finite k^* to 0 (see Fig. 8b further).

At small enough n , the region (ii) is no longer present: one then goes directly from region (i) to (iii) through a continuous decrease of the optimal stiffness k^* to 0. The intersection of $x_c(n)$ and $x_m(n)$ thus defines a tricritical point (x_t, n_t) , which we determine in the following.

4.1.1. Transition line $x_c(n)$

This position, when it exists, is defined by the equation

$$\left. \frac{\partial T_{II}(k, x_c)}{\partial k} \right|_{k=0} = 0. \quad (32)$$

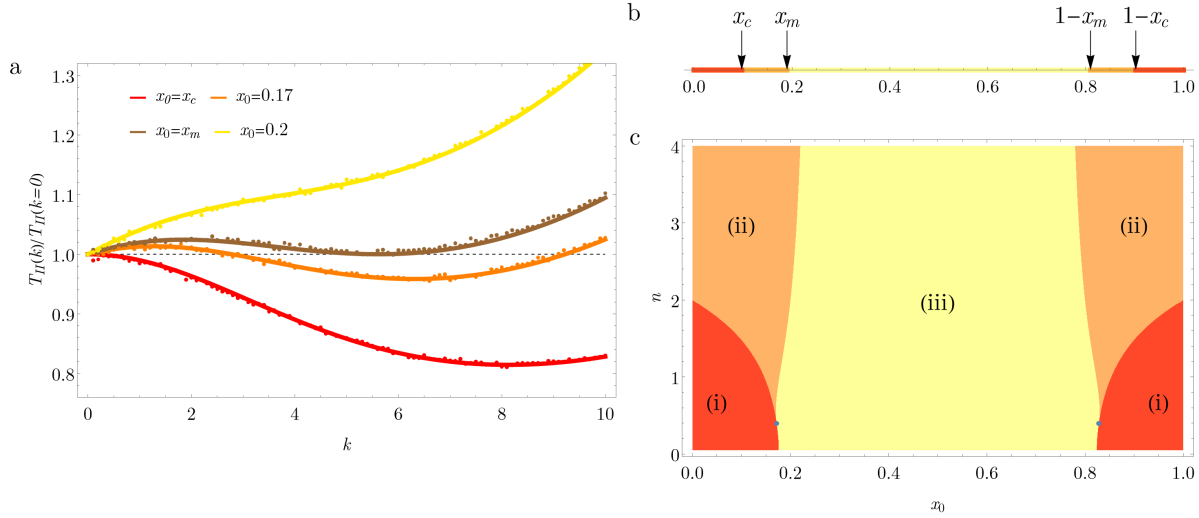


Figure 7. Mean exit time of a Brownian particle in set-up II, with a potential of the form $v(x) = k|x - x_0|^n/n$. The initial position of the particle is the potential minimum x_0 . (a) Ratio $T_{II}(k)/T_{II}(k=0)$ as a function of the potential stiffness k in the case $n = 1$, for different x_0 varied through the critical values $x_c \simeq 0.146447$ and $x_m \simeq 0.177311$. The latter position defines a discontinuous transition for the optimal parameter, from a value $k_{\text{opt}} \simeq 5.61157$ to $k_{\text{opt}} = 0$. Symbols represents Monte Carlo simulations; each point is an average over 2×10^5 realizations. (b) Position of the transitions points x_c , x_m and their symmetrical $1 - x_m$, $1 - x_c$, in the case $n = 1.5$. (c) Phase diagram in the (x_0, n) -plane. In region (i) in red, $dT_{II}/dk|_{k=0} \leq 0$ and the MFPT gets minimized at $k_{\text{opt}} > 0$. In region (ii) in orange, $dT_{II}/dk|_{k=0} > 0$ but the absolute minimum k_{opt} is still > 0 (metastable region). In region (iii) in yellow, simple diffusion becomes optimal ($k_{\text{opt}} = 0$). The three phases meet at the triple point $(0.17185, 0.39539)$ and its symmetrical $(0.82814, 0.39539)$

Taking the derivative of Eq. (31) and evaluating at $k = 0$ we obtain

$$\begin{aligned} \left. \frac{\partial T_{II}(k, x_c)}{\partial k} \right|_{k=0} &= \frac{1}{n} \frac{\int_0^1 dy \int_0^y dz}{\int_0^1 dy} \int_0^{x_c} dy |y - x_c|^n + \frac{1}{n} \frac{\int_0^1 dy \int_0^y dz (|y - x_c|^n - |z - x_c|^n)}{\int_0^1 dy} \int_0^{x_c} dy \quad (33) \\ &\quad - \frac{1}{n} \frac{\int_0^1 dy \int_0^y dz}{\left(\int_0^1 dy\right)^2} \int_0^{x_c} dy \int_0^1 dy |y - x_c|^n - \frac{1}{n} \int_0^{x_c} dy \int_0^y dz (|y - x_c|^n - |z - x_c|^n), \end{aligned}$$

which gives the following equation for x_c :

$$(n + 2 - 4x_c)x_c^n + (n - 2 + 4x_c)(1 - x_c)^n = 0. \quad (34)$$

The numerical resolution of Eq. (34) shows that when $0 < n < 2$, there exist two solutions in the interval $[0, 1]$: x_c and the symmetrical $1 - x_c$. For $n > 2$ the real solutions fall outside $[0, 1]$ and become unacceptable. It is remarkable that the transition between these two behaviors occurs for the generic harmonic potential $n = 2$, where Eq. (34) is easily solved, yielding $x_c = 0$ and 1 .

In the limit $n \rightarrow 0$ (corresponding to the logarithmic potential), one finds the non-trivial roots $x_c = 0.176041\dots$ and $1 - x_c = 0.823959\dots$.

4.1.2. Triple point

At the tricritical point, $x_c(n)$ and $x_m(n)$ intersect and the phases (i), (ii) and (iii) coexist. Hence, the condition (32) or (34) for $x_c(n)$ must be met. A second condition is deduced by noticing that, fixing n and varying x_0 , the transitions (ii)→(iii) and (i)→(iii) differ in the concavity of the MFPT at small k , which implies that $\partial_k^2 T_{II}|_{k=0} = 0$ right at the triple point separating them. More precisely, let us consider a point (x_0, n) in the vicinity of (x_t, n_t) and expand T_{II} in powers of k :

$$T_{II}(k) = T_0 + ak + bk^2 + dk^3 + \dots, \quad (35)$$

with $d > 0$. In the metastable region (ii), $a > 0$ and as k increases from 0 the MFPT has a local maximum before reaching its global minimum. This implies that $b < 0$. Across the transition (i)→(iii), on the other hand, a changes sign. Let us assume that $b < 0$ in this case, too, and show that this leads to a contradiction. Consider a point in the region (iii) very close to the phase (i), *i.e.*, $a > 0$ but arbitrarily small. Solving $\partial_k T_{II}(k) = 0$ gives the local minimum $k^* \simeq -\frac{2b}{3d} + \frac{a}{2b}$ and $T(k^*) \simeq T_0 + \frac{20b}{27d^2} - 2ab \simeq T_0 + \frac{20b}{27d^2} < T_0$ since $b < 0$. Hence T_0 is not the absolute minimum, which contradicts the definition of phase (iii). Therefore b is positive across the transition (i)→(iii). By continuity, b must vanish at the triple point, or

$$\left. \frac{\partial^2 T_{II}(k, x_t)}{\partial k^2} \right|_{k=0} = 0. \quad (36)$$

The tricritical point (x_t, n_t) is thus a point of inflection where both $\partial_k T_{II}$ and $\partial_k^2 T_{II}$ vanish at $k = 0$. The second condition is obtained from deriving Eq. (31) twice. After a lengthy calculation, one obtains

$$\begin{aligned} \left. \frac{\partial^2 T_{II}}{\partial k^2} \right|_{k=0} = & \frac{x_0(1-x_0)^{2n+1}}{(n+1)^2(2n+1)} + \frac{x_0(1-x_0)(x_0^n - (1-x_0)^n)}{n^2} \left(\frac{x_0^n + (1-x_0)^n}{2(2n+1)} \right. \\ & - \frac{4x_0^2(x_0^n - (1-x_0)^n) - (n-2)(1-x_0)^n}{(n+1)^2(n+2)} \\ & \left. - \frac{2x_0[(n+2-4x_0)x_0^n + (n-2+4x_0)(1-x_0)^n]}{(n+1)^2(n+2)} \right). \end{aligned} \quad (37)$$

Setting the above expression to zero and combining it with Eq. (34) boils down to the rather simple system

$$(n+2-4x_0)x_0^n + (n-2+4x_0)(1-x_0)^n = 0, \quad (38)$$

$$(n+2)[(n-4)n+2] + 16(n-1)(1-x_0)x_0 = 0, \quad (39)$$

whose numerical solution in the interval $x_t < 1/2$ is

$$n_t = 0.395391\dots \quad (40)$$

$$x_t = 0.171859\dots \quad (41)$$

The second triple point is at $(n_t, 1-x_t)$ by symmetry.

4.2. Comparison with optimal resetting

The case $n = 1$, which is the closest to diffusion with stochastic resetting, exhibits four transitions as x_0 is varied in the phase diagram 7b. In the resetting problem with the same set-up, however, there are only two transition points, as the metastable behaviour leading to region (ii) is absent. With two absorbing boundaries, the mean exit time T_r of a Brownian particle subject to resetting to the initial position can be calculated following the same route as in section 3.2 with $c = 1$ (see also [38]):

$$T_r = \frac{1}{r} \left(\frac{\sinh \sqrt{r}}{\sinh(1-x_0)\sqrt{r} + \sinh x_0\sqrt{r}} - 1 \right). \quad (42)$$

When the resetting rate r is varied at fixed x_0 , the MFPT above exhibits only one local minimum, at $r = 0$ or at a finite value. The transition occurs when $\partial_r T_r|_{r=0} = 0$, which gives $x_{c,r} = (5 - \sqrt{5})/10 = 0.27639\dots$ (symmetrically the second transition occurs at $1 - x_{c,r} = (5 + \sqrt{5})/10$) [38].

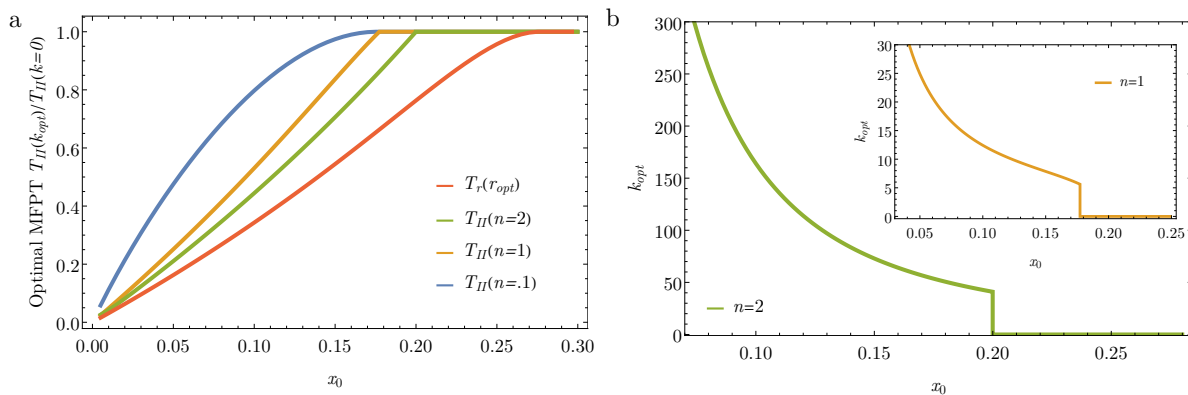


Figure 8. (a) Mean absorption time of a Brownian particle in set-up II in the presence of an external potential of the form $v(x) = k|x - x_0|^n/n$ at $k = k_{opt}$, or under the action of stochastic resetting at $r = r_{opt}$ (red curve). Searches start from the resetting/potential minimum position x_0 . The times are normalized by the free diffusion MFPT for each x_0 . (b) Optimal stiffness as a function of x_0 . In the harmonic case $n = 2$, the discontinuous transition occurs at $x_m = 0.199951\dots$, and for $n = 1$, at $x_m = 0.177311\dots$

Fig. 8a depicts the optimal MFPTs obtained by minimizing Eq. (42) with respect to r at fixed x_0 , as well as the ones corresponding to several optimal potentials. These times are normalized by the free-diffusion MFPT ($r = 0$ or $k = 0$) for each x_0 . Once again, optimal resetting is always more efficient than the optimal equilibrium dynamics. Both processes, however, become much more efficient than free diffusion as x_0 gets closer to one of the targets.

Further analysis of Eq. (42) shows that $\partial_r^2 T_r|_{r=0} > 0$, which implies that the freezing transition between the regimes $r_{opt} = 0$ and $r_{opt} > 0$ is continuous, in contrast with the discontinuous behavior of k_{opt} in the potential case when $n > n_t$. This is confirmed by Fig. 8b, where the optimal parameter k_{opt} for $n = 1$ or 2 jumps from a non-zero value to 0 when x_0 crosses x_m from below.

5. Discussion

We have computed the mean first passage time of a one-dimensional Brownian particle to an absorbing boundary in the interval $[0, c]$, in the presence of an external confining potential of the form $v(x) = k|x - x_0|^n/n$, where $x_0 \in [0, c]$ is also the starting position. When an absorbing boundary is placed at the origin and a reflective wall at c , the search time can be minimized by a suitable choice of the potential stiffness k . The optimal stiffness k_{opt} undergoes a second order "freezing" transition as the relative distance c/x_0 crosses a critical number $c^*(n)$, which depends on n . When $c/x_0 > c^*(n)$, the additional confinement produced by the potential can help complete the search process faster, or $k_{\text{opt}} > 0$. Otherwise, search is delayed by the potential, or $k_{\text{opt}} = 0$.

This freezing transition is analogous to the one observed in a non-equilibrium situation, *i.e.*, a diffusive process with stochastic resetting to the starting position. In this case the resetting rate r plays a role analogous to k^2 in the case $n = 1$. Below a relative domain size $c/x_0 = c_r^*$, stochastic resetting is no longer beneficial either compared to simple diffusion, but the critical number c_r^* is smaller than $c^*(n)$ for all n . Hence, compared to any optimal equilibrium situation, optimal resetting processes not only allow faster target encounters but they are also useful in smaller domains.

When both ends of the interval are absorbing, the optimization of the MFPT is more intricate. Setting $c = 1$ for convenience, we found the existence of three different "phases" in the (x_0, n) -plane for which the behaviour of the MFPT is completely different. In the phase (i), the MFPT decreases with increasing k from zero and reaches a minimum at a non-zero potential stiffness. In the phase (ii), the MFPT is metastable: it first increases with k , goes through a local maximum and then decreases to reach a global minimum at $k_{\text{opt}} > 0$, like in phase (i). In the phase (iii), pure diffusion is optimal ($k_{\text{opt}} = 0$). For the transition (i) \rightarrow (iii) the optimal stiffness undergoes a continuous transition. In contrast, the transition (ii) \rightarrow (iii) is discontinuous. Somehow unexpectedly, region (i) disappears for potentials with $n \geq 2$: in other words, the additional confinement produced by a weak harmonic (or higher order) potential will always delay absorption compared to simple diffusion, independently of the starting position/domain size.

Notably, there are two symmetrical tricritical points in the (x_0, n) -plane, at which the three above phases coexist: for a potential exponent $n < n_t = 0.395391\dots$, the system can only be in the phases (i) and (iii). For $n = 1$, which is above n_t , there are four transitions as x_0 is varied. This behaviour of the MFPT is not observed for a diffusive process with stochastic resetting to the origin, where the transitions in the optimal resetting rate are continuous and where the absence of metastability effects limits the number of dynamical phases to two.

The study of optimal searches under stochastic resetting to the initial position is simplified by the existence of a universal criterion, valid for any background process [38, 45–48]. The criterion tells that if the coefficient of variation (*CV*) of the first passage times of the underlying process (without resetting) is larger than unity, then resetting will produce a speed-up of the search process. Otherwise, resetting will be detrimental.

Hence, the transition points c_r^* (in set-up I) or $x_0 = x_{c,r}$ (in set-up II) are such that the CV corresponding to free Brownian motion is exactly 1. Similarly, it would be useful to predict whether an external potential can decrease or not the mean search time, based only on a property of the process without potential. However, no such universal relation exists in this case. This can be seen by noticing that the transition points $c^*(n)$ or $x_c(n)$ depend on n , *i.e.*, on the shape of the potential that is going to be applied. As $c^*(n)$ varies between 2 and 2.42153... in set-up I (see also Fig. 3), it is unlikely that a Brownian quantity related to a first passage time remains constant in this range. However we can make a few general statements: as mentioned above, with two absorbing boundaries, harmonic potentials of weak stiffness cannot improve the mean absorption time, while weak piece-wise linear potentials can.

Our study also shows that one should be cautious in drawing conclusions about the negative effects on the MFPT of an increasing potential strength (or resetting rate), based on a perturbative analysis of the free diffusion case. Such analysis, which leads to the general criteria $CV = 1$ mentioned above for resetting processes, does not guarantee that an absolute minimum does not exist for a large value of the parameter considered, out of the regime of validity of the calculation. Metastable minima of the MFPT analogous to the ones found here by varying k were recently observed with respect to the resetting rate for a Brownian particle in a bounded domain and subject to different potential shapes [41]. In that study, the number of absorbing boundaries also played a crucial role on the order of the transition for the optimal resetting rate. With two absorbing walls, tricritical points were usually present. Similar transitions have been found in drift-diffusion processes and Michaelis-Menten chemical reactions with restart [49].

Metastability in the mean first passage time was also observed experimentally and theoretically for a free Brownian particle under resetting to a distribution of resetting positions, given by the Boltzmann-Gibbs distribution in a harmonic potential [50–52]. When the distance to the target is of the order of the width of this distribution, the MFPT exhibits a metastable behavior as the resetting periodicity is varied. These results were further generalized to the case of a one-dimensional persistent random walks in a harmonic potential, for which the distribution of resetting positions is non-Boltzmann [53]. Metastability is also the outcome of other protocols that use intermittent potentials to mimic non-ideal resetting processes [54].

To summarize, we have studied under which circumstances the application of an external confining potential acting on a Brownian particle in a bounded domain enhances target encounter, or when it is more convenient to let the particle diffuse without any external forces. Our analysis reveals some intricate effects of the potential shape on the optimal search strategy. This calls for seeking new optimal protocols that employ confining potentials in bounded or infinite domains, for instance potentials that fluctuate in time [21, 54, 55].

Acknowledgments

GMV thanks CONACYT (Mexico) for a scholarship support. We acknowledge support from Ciencia de Frontera 2019 (CONACYT), project “Sistemas complejos estocásticos: Agentes móviles, difusión de partículas, y dinámica de espines” (Grant 10872).

References

- [1] Van Kampen N G 1992 *Stochastic processes in physics and chemistry* vol 1 (Elsevier)
- [2] Redner S 2001 *A Guide to First-Passage Processes* (Cambridge University Press)
- [3] Bray A J, Majumdar S N and Schehr G 2013 *Advances in Physics* **62** 225–361
- [4] Szabo A, Schulten K and Schulten Z 1980 *The Journal of Chemical Physics* **72** 4350–4357
- [5] Cui T, Ding J and Chen J Z Y 2006 *Macromolecules* **39** 5540–5545
- [6] Zhang Y and Dudko O K 2016 *Annual Review of Biophysics* **45** 117–134
- [7] Chou T and D’Orsogna M R 2014 First passage problems in biology *First-Passage Phenomena and Their Applications* (World Scientific) pp 306–345
- [8] Gerstein G L and Mandelbrot B 1964 *Biophysical journal* **4** 41–68
- [9] Beggs J M and Plenz D 2003 *Journal of Neuroscience* **23** 11167–11177 ISSN 0270-6474
- [10] Viswanathan G M, da Luz M G E, Raposo E P and Stanley H E 2011 *The Physics of Foraging: An Introduction to Random Searches and Biological Encounters* (Cambridge University Press)
- [11] Kagan E and Ben-Gal I 2015 *Search and Foraging: Individual Motion and Swarm Dynamics* (CRC Press) ISBN 9781482242096
- [12] Chicheportriche R and Bouchaud J P 2014 Some applications of first-passage ideas to finance *First-passage Phenomena And Their Applications* (World Scientific) pp 447–476
- [13] Bénichou O, Chevalier C, Klafter J, Meyer B and Voituriez R 2010 *Nature chemistry* **2** 472–477
- [14] Bénichou O and Voituriez R 2014 *Physics Reports* **539** 225–284 ISSN 0370-1573 from first-passage times of random walks in confinement to geometry-controlled kinetics
- [15] Bénichou O and Voituriez R 2008 *Phys. Rev. Lett.* **100**(16) 168105
- [16] Bamford C, Tipper C and Compton R 1985 *Diffusion-Limited Reactions, Comprehensive Chemical Kinetics Vol. 25* (Elsevier)
- [17] Chevalier C, Bénichou O, Meyer B and Voituriez R 2010 *Journal of Physics A: Mathematical and Theoretical* **44** 025002
- [18] Kramers H A 1940 *Physica* **7** 284–304
- [19] Hänggi P, Talkner P and Borkovec M 1990 *Rev. Mod. Phys.* **62**(2) 251–341
- [20] Sabhapandit S and Majumdar S N 2020 *Phys. Rev. Lett.* **125**(20) 200601
- [21] Doering C R and Gadoua J C 1992 *Phys. Rev. Lett.* **69**(16) 2318–2321
- [22] Palyulin V V and Metzler R 2012 *Journal of Statistical Mechanics: Theory and Experiment* **2012** L03001
- [23] Chupeau M, Gladrow J, Chepelianskii A, Keyser U F and Trizac E 2020 *Proceedings of the National Academy of Sciences* **117** 1383–1388
- [24] Palyulin V V and Metzler R 2013 *Journal of Physics A: Mathematical and Theoretical* **47** 032002
- [25] Kuśmierz Ł, Bier M and Gudowska-Nowak E 2017 *Journal of Physics A: Mathematical and Theoretical* **50** 185003
- [26] Evans M R and Majumdar S N 2011 *Phys. Rev. Lett.* **106**(16) 160601
- [27] Evans M R and Majumdar S N 2011 *Journal of Physics A: Mathematical and Theoretical* **44** 435001
- [28] Evans M R, Majumdar S N and Schehr G 2020 *Journal of Physics A: Mathematical and Theoretical* **53** 193001
- [29] Kuśmierz Ł, Majumdar S N, Sabhapandit S and Schehr G 2014 *Phys. Rev. Lett.* **113**(22) 220602
- [30] Manrubia S C and Zanette D H 1999 *Phys. Rev. E* **59**(5) 4945–4948

- [31] Evans M R and Majumdar S N 2018 *Journal of Physics A: Mathematical and Theoretical* **52** 01LT01
- [32] Majumdar S N, Sabhapandit S and Schehr G 2015 *Phys. Rev. E* **91**(5) 052131
- [33] Gupta D, Pal A and Kundu A 2021 *Journal of Statistical Mechanics: Theory and Experiment* **2021** 043202
- [34] Singh P 2020 *Journal of Physics A: Mathematical and Theoretical* **53** 405005
- [35] Evans M R, Majumdar S N and Mallick K 2013 *Journal of Physics A: Mathematical and Theoretical* **46** 185001
- [36] Giuggioli L, Gupta S and Chase M 2019 *Journal of Physics A: Mathematical and Theoretical* **52** 075001
- [37] Christou C and Schadschneider A 2015 *Journal of Physics A: Mathematical and Theoretical* **48** 285003
- [38] Pal A and Prasad V V 2019 *Phys. Rev. E* **99**(3) 032123
- [39] Singh R K, Metzler R and Sandev T 2020 *Journal of Physics A: Mathematical and Theoretical* **53** 505003
- [40] Ray S and Reuveni S 2021 *The Journal of Chemical Physics* **154** 171103
- [41] Ahmad S, Rijal K and Das D 2022 *Phys. Rev. E* **105**(4) 044134
- [42] Ahmad S, Nayak I, Bansal A, Nandi A and Das D 2019 *Phys. Rev. E* **99**(2) 022130
- [43] Risken H 1996 Fokker-planck equation *The Fokker-Planck Equation* (Springer)
- [44] Gardiner C 2004 *Handbook of Stochastic Methods for Physics, Chemistry, and the Natural Sciences* Springer complexity (Springer) ISBN 9783540208822
- [45] Reuveni S 2016 *Phys. Rev. Lett.* **116**(17) 170601
- [46] Pal A and Reuveni S 2017 *Phys. Rev. Lett.* **118**(3) 030603
- [47] Belan S 2018 *Phys. Rev. Lett.* **120**(8) 080601
- [48] Ray S, Mondal D and Reuveni S 2019 *Journal of Physics A: Mathematical and Theoretical* **52** 255002
- [49] Pal A and Prasad V V 2019 *Phys. Rev. Research* **1**(3) 032001
- [50] Besga B, Bovon A, Petrosyan A, Majumdar S N and Ciliberto S 2020 *Phys. Rev. Research* **2**(3) 032029
- [51] Besga B, Faisant F, Petrosyan A, Ciliberto S and Majumdar S N 2021 *Phys. Rev. E* **104**(1) L012102
- [52] Faisant F, Besga B, Petrosyan A, Ciliberto S and Majumdar S N 2021 *Journal of Statistical Mechanics: Theory and Experiment* **2021** 113203
- [53] Tucci G, Gambassi A, Majumdar S N and Schehr G 2022 *arXiv preprint arXiv:2203.16066*
- [54] Mercado-Vásquez G, Boyer D, Majumdar S N and Schehr G 2020 *Journal of Statistical Mechanics: Theory and Experiment* **2020** 113203
- [55] Capała K, Dybiec B and Gudowska-Nowak E 2021 *Chaos: An Interdisciplinary Journal of Nonlinear Science* **31** 063123